ELSEVIER

Applied Catalysis A: General 167 (1998) 173–181

APPLIED CATALYSIS A: GENERAL

Physico-chemical and MAS NMR characterization of mesoporous SAPOs

Basab Chakraborty, Alex C. Pulikottil, B. Viswanathan*

Department of Chemistry, Indian Institute of Technology, Madras 600036, India

Received 9 June 1997; received in revised form 29 September 1997; accepted 29 September 1997

Abstract

Mesoporous SAPOs (average pore radius ~30 Å) have been synthesized using organized micellar arrays of templates. The synthesized SAPOs have been characterized by XRD, TEM, TGA, sorption and MAS NMR techniques. There is no evidence of Si–O–P linkages in these materials. The distribution of silicon around Al ions was studied by calcination at higher temperatures. The possibility of synthesizing mesoporous SAPOs with silicon rich regions, possessing lesser acidity than the zeolites, will open up new avenues for their technical applications. © 1998 Elsevier Science B.V.

Keywords: Silicoaluminophosphate; Mesoporous; Characterization; Magnetic angle spinning; NMR

1. Introduction

The development of aluminophosphate-based materials has extended the compositional and structural diversity of molecular sieve materials. Substitution of silicon for P in aluminophosphates results in charge imbalance in the framework, thereby generating acidity in these materials. They exhibit characteristic properties of zeolites and of aluminophosphate in addition to the properties ascribable to their compositions.

The studies on phosphate-based molecular sieves have led to the synthesis of large pore materials, thus breaking the conventional 12 T atom ring barrier of the molecular sieves. Davis et al. [1] have reported the synthesis of VPI-5, an aluminophosphate-based molecular sieve comprising 18-membered rings. Recently a 20-membered ring aluminophosphate, viz. JDF-20 has been synthesized [2]. Although these materials have large porous texture, their pore openings do not exceed 10–12 Å.

The discovery of M41S family of molecular sieves by the Mobil group [3] has led to the synthesis of various materials having pores in the mesoporous range. These syntheses were based on the cooperative assembly of periodic inorganic matrices over organic surfactants. Recently this novel approach has been extended by us for the first time for synthesizing silicoaluminophosphates (SAPO) in the mesoporous range [4]. The applicational utility of these new class of materials depends on their thermal stability as well as their surface acidic/basic properties. The objectives of the present study are to find out (I) whether silicon substitutes for aluminium or phosphorous or both in these SAPO materials and (II) whether there is any systematic ordering of silicon in certain regions of

*Corresponding author. Fax. 00 91 44 235 0509

PII S0926-860X(97)00319-0

these materials. There is yet another aspect which has not been addressed in this paper: if there were to be some accumulation of silicon-rich regions, then these materials can be exploited for a variety of applications like preferential adsorption, selective surface migration and reaction (surface dynamics) and also polyfunctionality in catalysis. For embarking on exploitation of these materials for these selective applications, it is necessary to characterize these materials at molecular level. Hence, in this paper the thermal stability of the framework and the local environment of silicon incorporated have been examined in detail using solid state MAS NMR technique on these mesoporous SAPO materials calcined at different temperatures.

2. Experimental

The mesoporous SAPOs were prepared using aluminum isopropoxide (Loba Chemie), phosphoric acid (Merck) and tetraethyl orthosilicate (TEOS) (Merck) as the sources of aluminum, phosphorous and silicon respectively. Cetyltrimethyl ammonium bromide (CTAB) was employed as a template in the synthesis. In a typical synthesis, 8 g of aluminum isopropoxide was mixed with dilute phosphoric acid (6.2 ml of H_3PO_4 in 60 ml of H_2O). The resultant mixture was stirred vigorously for 1 h at 333 K. CTAB (8 g in 20 ml H_2O) was then added, with subsequent addition of appropriate amounts of tetraethyl orthosilicate dissolved in 4 ml of tetramethyl ammonium hydroxide; the resulting gel was stirred for another 1 h. The pH of the resulting gel was around 2.5. The molar composition of the gel thus obtained was: $71.2P_2O_5$: $26.8Al_2O_3$:$1.0SiO_2$:31.5CTAB:$6082H_2O$

The gel was autoclaved for 48 h at 383 K without stirring. The autoclaved material was cooled and the crystalline products were filtered, washed several times with hot water and dried in an air oven at 383 K for 12 h. After crystallization, the pH of the mother liquor increased to 7. Different amounts of silicon were incorporated by varying the amounts of TEOS in the preparation medium. Samples were calcined initially in nitrogen atmosphere for 1 h at 873 K, followed by heating in air for 12 h.

All samples were characterized using XRD, TGA, TEM, sorption studies and solid state MAS NMR measurements. X ray diffractograms were recorded in Rich Seifert XRD 3000P instrument using Cu Kα radiation (35 KV, 30 mA, $2°min^{-1}$). Thermogravimetric analyses of the uncalcined samples were carried out using Perkin Elmer TGA (Delta series TGA7) instrument with a heating rate of 20 K min^{-1}. TEM studies were carried out in Philips CM12 scanning transmission electron microscope operating at 100 KV. The powdered samples were supported on carbon coated copper grids. Adsorption isotherms were determined at 77 K using a Carlo Erba sorptomatic series 1800 instrument using nitrogen as the adsorbent. MAS NMR spectra were recorded using Jeol GSX400 instrument. The Larmor frequencies were 104.1, 161.8 and 79.4 MHz for ^{27}Al, ^{31}P and ^{29}Si respectively. Tetramethyl silane, 85% phosphoric acid, and a solution of aluminum nitrate were used as references for ^{29}Si, ^{31}P and ^{27}Al respectively. Data were acquired at an MAS speed of 5.5 KHz. All the samples are exposed to atmosphere at room temperature and hydrated before recording the NMR spectra.

3. Results and discussion

X-ray diffractograms of all the calcined samples of mesoporous silicoaluminophosphates (SAPO) are shown in Fig. 1. The low angle peaks exhibited by all the samples in the XRD patterns are typical of mesoporous materials [3]. The low angle peaks are indexed on the basis of hexagonal symmetry. The d_{100} values for all the samples along with the lattice parameter 'a' are given in Table 1. However the peaks occuring at higher 2θ values could not be indexed. The synthesized materials are found to be less crystalline compared to the known SAPOs. Also a loss in crystallinity is observed on calcining these samples.

Table 1
The molar ratios of the synthesis gel and that of the samples as obtained from elemental analysis along with d_{100} line spacings and the lattice parameter 'a' of the samples

Sample	Al/P molar ratio		Al/Si molar ratio		d_{100} (Å)	a (Å)
	Gel	As syn.	Gel	As syn.		
S-I	0.38	0.81	87.1	90.02	28.14	32.49
S-II	0.38	1.01	53.7	61.04	28.28	32.65
S-III	0.38	1.13	29.3	34.80	28.44	32.84

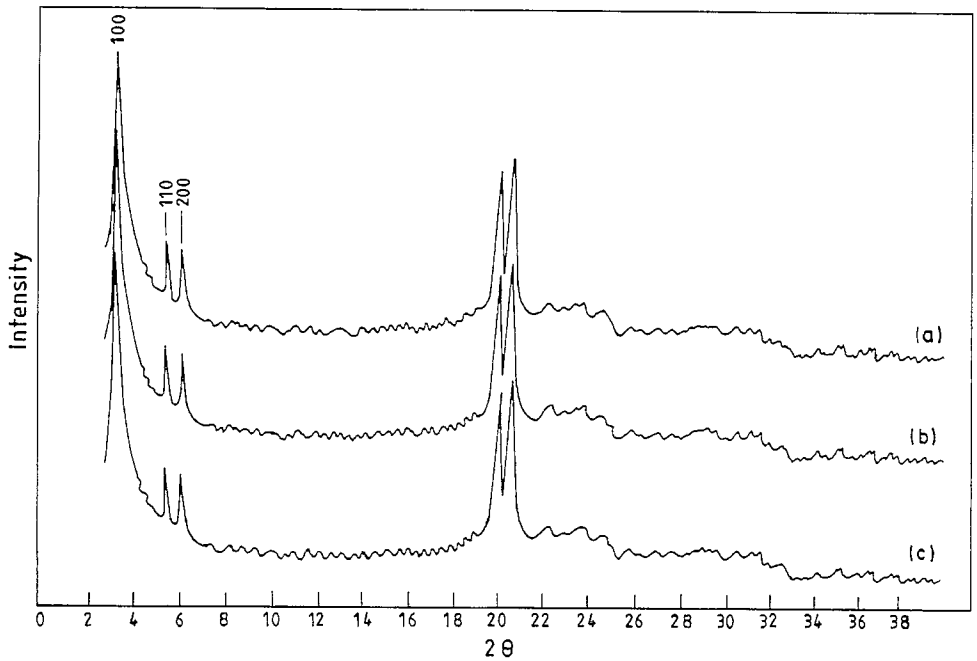

Fig. 1. XRD pattern of calcined (a) S-I (b) S-II and (c) S-III samples.

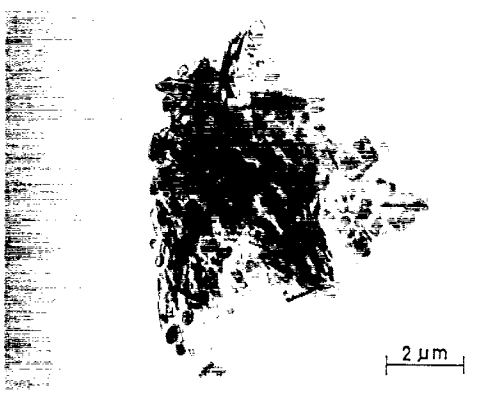

Fig. 2. Transmission electron micrograph of the calcined S-II sample.

Transmission electron micrographs (Fig. 2) of the calcined S-II sample indicate the faceted nature of the synthesized crystals of SAPO. The two-dimensional projected image of the TEM photographs reveal the hexagonal external morphology of the crystals. The crystals are also found to grow along a particular direction, probably along the most densely packed plane. The average size of the crystals is found to be 50–75 nm.

The chemical analysis results of the synthesized materials given in Table 1 show that some but not all of the silica in the original gel is incorporated in the synthesized materials. No change in phases or appearance of any new phase is observed in the XRD pattern and in the TEM micrographs with increase in silica content of the synthesized SAPO materials.

Thermogravimetric analysis of the as-synthesized SAPO samples exhibit characteristic weight losses in three stages (Fig. 3). The total weight loss of the as-synthesized sample corresponds to 30%. The initial weight loss due to water occurs in the range 493–513 K (11%). Subsequent weight losses occurring in the range of 573–593 K are assigned to loss of weakly bound template and that at 873 K to a template strongly interacting with the molecular sieve. Thus, a strong bonding interaction between the organic surfactant and the inorganic matrix is observed. Hence, to avoid crystallinity loss, these SAPO materials are to be calcined initially in nitrogen atmosphere at 873 K, followed by calcination in air.

Low temperature nitrogen adsorption isotherms provide reliable information on the mesoporous structure of these materials. Fig. 4 shows the N_2 adsorption isotherm for the S-II sample. This is a

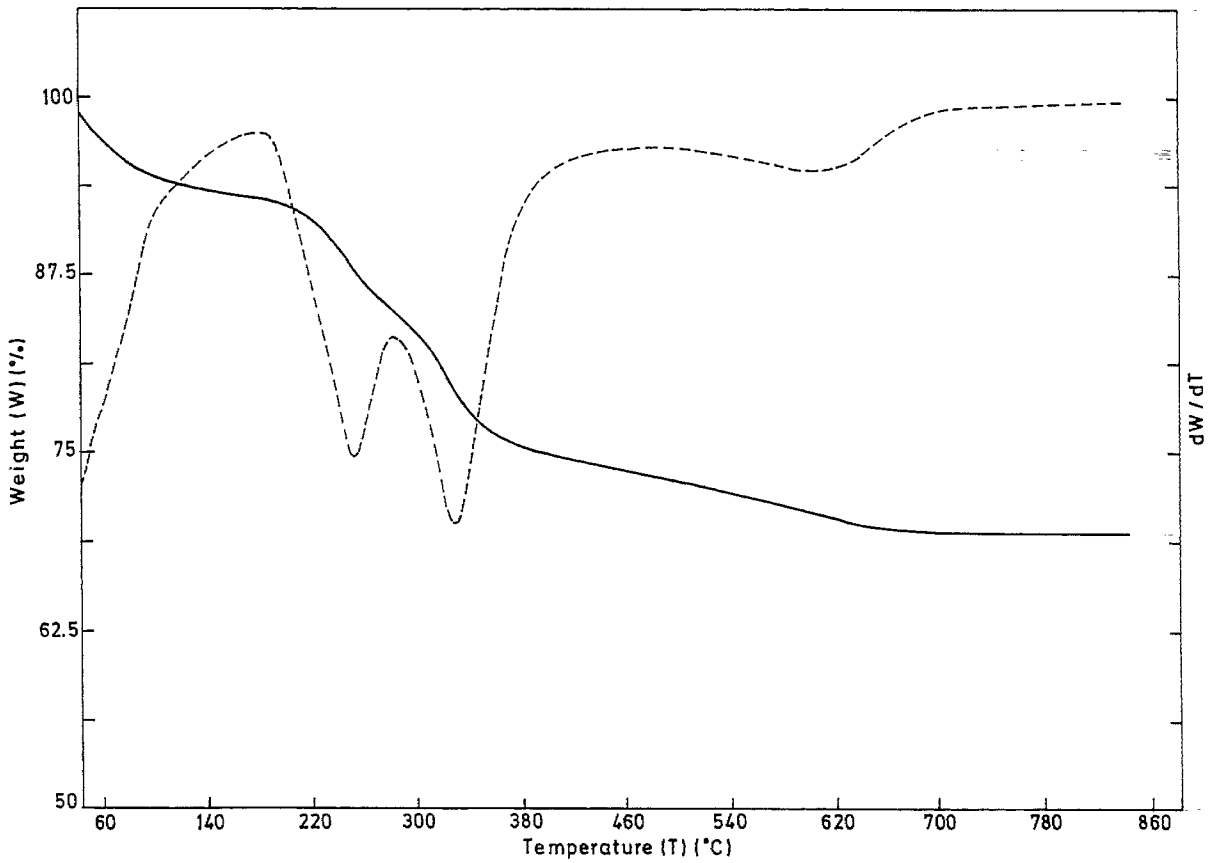

Fig. 3. TGA(—) and DTG(– – –) curves of the as-synthesized S-II sample.

typical irreversible type IV isotherm with a hysteresis loop. Adsorption at low relative pressures (P/P^0<0.3) is due to the monolayer adsorption of N_2 on the mesoporous walls. With increase in the relative pressure, the isotherm is marked by a sharp inflection characteristic of capillary condensation within the uniform mesopores, the P/P^0 position being related to the diameter of the mesopores. Moreover, the sharp inflection in this step indicates the uniformity of the mesopores. Also, the broad hysteresis loop in the isotherm confirms the presence of uniform mesopores in these materials. This type of isotherm is also found in the mesoporous MCM41 materials [5]. The pore size distribution computed on the basis of BJH analysis indicates a remarkably narrow distribution, with the maximum centered around 30 Å for all the samples, reflecting a uniform pore texture of the samples (Fig. 5). All the samples were found to exhibit high surface areas, around 900 m^2gm^{-1}.

3.1. ^{31}P MAS NMR

Fig. 6 shows the ^{31}P MAS NMR spectra of S-II sample calcined at different temperatures. The ^{31}P MAS NMR of the as-synthesized S-II sample shows two peaks centered at −31.0 and −21.1 ppm (Fig. 6(a)). The high intense peak at −31.0 ppm can be assigned to P(4Al) environment which is common for other known SAPOs [6]. The additional low intensity peak having a shift towards that of free phosphoric acid suggests that these PO_4 tetrahedra are not completely linked with AlO_4 tetrahedra. These P atoms are linked to hydroxyl groups also. An enhancement in the intensity of the peak at −21.1 ppm is observed in a ^{31}P CP MAS NMR study

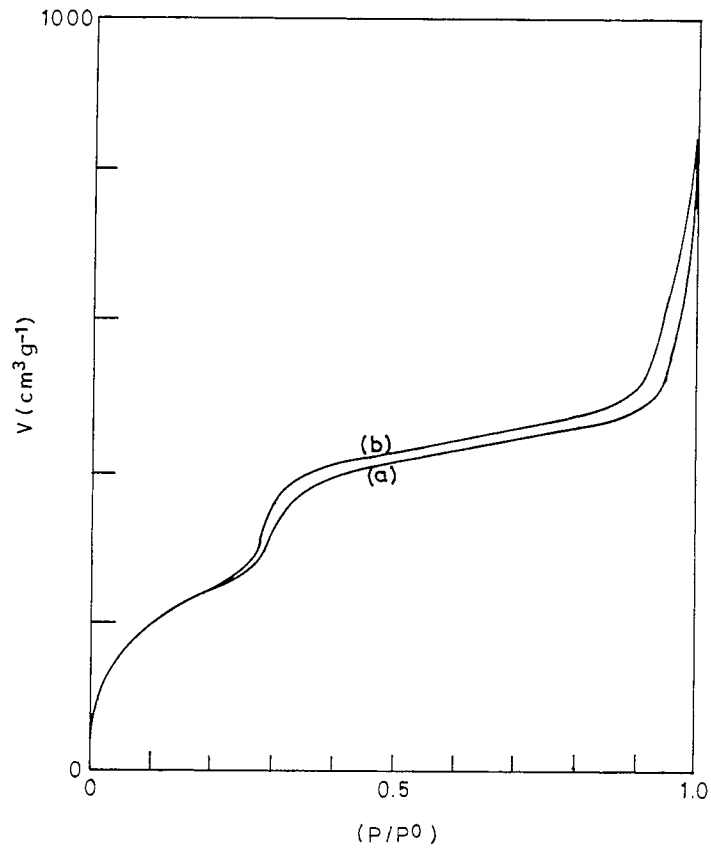

Fig. 4. Adsorption (a) and desorption (b) isotherms of nitrogen for calcined S-II sample.

(Fig. 6(a′)). This indicates that the environment around P is P(3Al,1OH). Jahn et al. [6] observed similar shifts in ^{31}P NMR spectra of SAPO-11 samples. However with calcination the intensity of the peak at −21.1 ppm gradually decreased till 773 K (Fig. 6(a)–(e)), above which there is no trace of the defect sites at 873 K. In the sample calcined at 873 K, only one environment, viz. P(4Al), exists (Fig. 6(f)). Similar observations were found for the ^{31}P MAS NMR of S-I and S-III samples (Fig. 7). It is to be noted that a single large resonance at −31.0 ppm was observed for all the samples irrespective of the amount of Si present. This indicates that P–O–Si linkages are probably absent in these mesoporous SAPOs and/or there is no influence of this linkage on the NMR spectra. It is documented in the literature that P–O–Si linkages are absent in known SAPOs. Thus it can be deduced that silicon substitutes for the phosphorous site and not for the aluminium site.

3.2. ^{27}Al MAS NMR

The ^{27}Al MAS NMR spectra of S-II sample are shown in Fig. 8. The uncalcined sample showed two peaks at 36.6 and 6.2 ppm. The resonance at 36.6 ppm is characteristic of Al in the framework tetrahedral environment in SAPOs [7,8]. The peak at 6.2 ppm can be assigned to Al in higher coordination. The intensity of the peak at 6.2 ppm due to framework Al coordinated with two water molecules and/or template species at low temperature gradually decreased with calcination till 773 K (Fig. 8(a)–(e)). At 873 K, the defect sites completely disappeared (Fig. 8(f)). Similar signals were observed for S-I and S-III samples with slight shifts (Fig. 9). Thus S-I sample having the least Si has the resonance centered around 36.0 ppm, followed by S-II sample at 36.6 ppm; S-III having the maximum Si incorporation gives the chemical shift at 37.2 ppm. It was found that with increase in Si con-

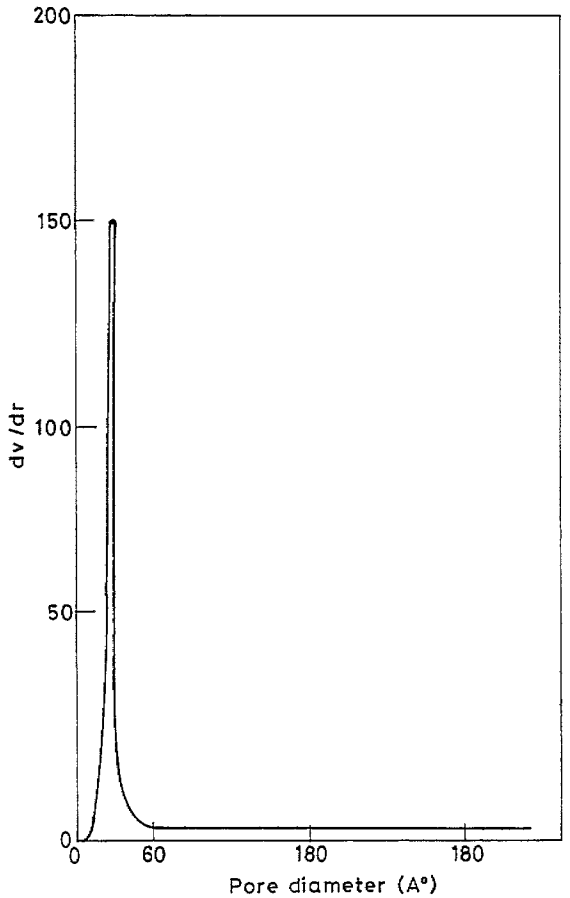

Fig. 5. Pore size distribution curve of the S-II sample calculated from the desorption branch of the nitrogen adsorption isotherm using the BJH formula.

centration the peak due to tetrahedral Al shifted slightly to the higher field values. The change in chemical shift might be due to the increasing interactions of Al with Si atoms with increase in Si incorporation from S-I to S-III sample.

3.3. ^{29}Si MAS NMR

The ^{29}Si MAS NMR spectra for S-II sample calcined at different temperatures are shown in Fig. 10. All the spectra show peaks centered at −107.5, −104, −98, −95 and −90 ppm. Based on the assignments by various authors [9,10], the above peaks are assigned as follows: −90 ppm to Si(4Al), −95 ppm to Si(3Al), −98 ppm to Si(2Al), −104 ppm to Si(1Al) and −107.5 ppm to Si(0Al). With calcination, the

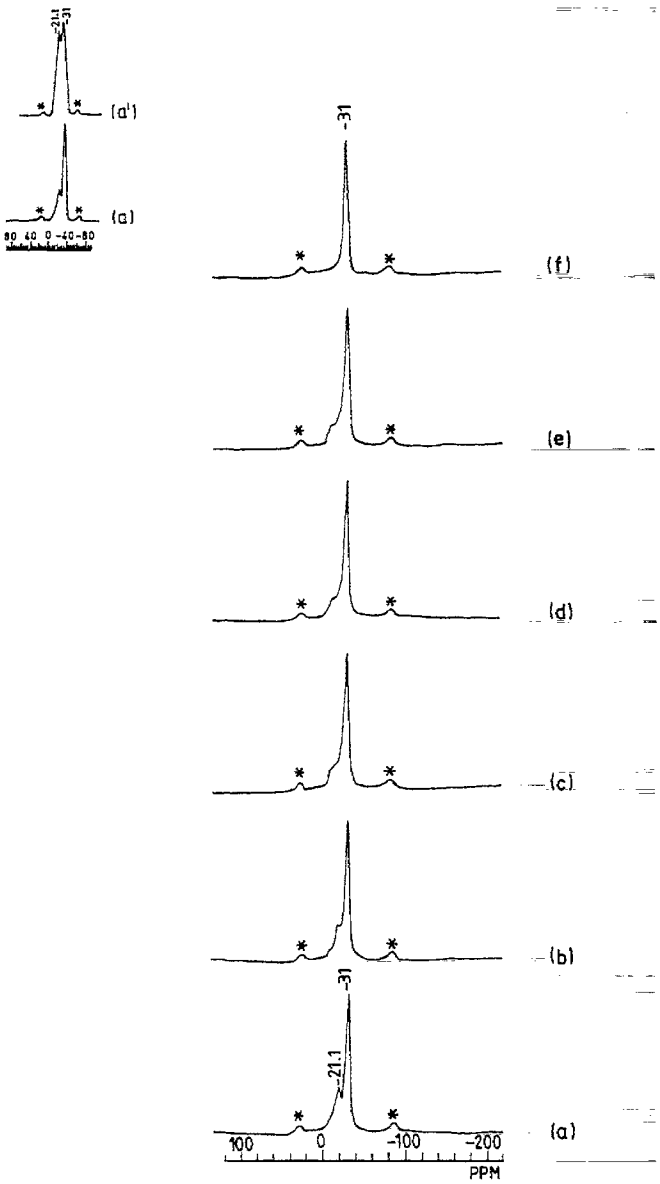

Fig. 6. ^{31}P MAS NMR spectra of S-II sample calcined at different temperatures: (a) as-synthesized, (b) 473 K, (c) 573 K, (d) 673 K, (e) 773 K, (f) 873 K; Inset: same as (a) and (a′) is ^{31}P CP MAS NMR spectra of the as-synthesized S-II sample. * indicates spinning sidebands.

intensity of the peak at −90 ppm decreases and that of the peak at −104 ppm increases to a maximum. This implies that, with calcination, Si-rich regions predominate. In S-III sample (Fig. 11) the least Si is present in Si(4Al) environment in the calcined

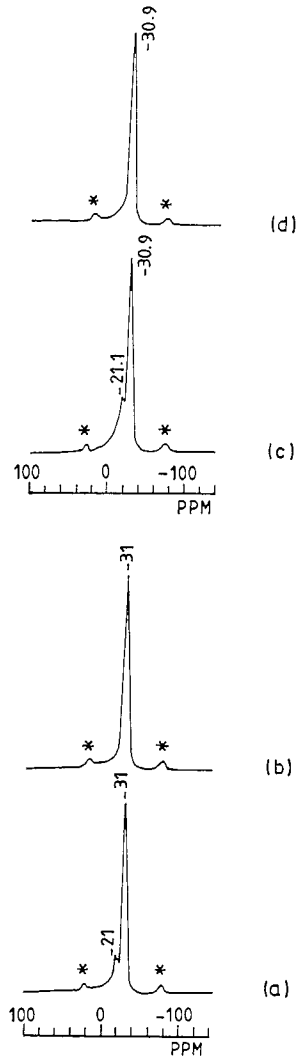

Fig. 7. ^{31}P MAS NMR spectra of S-I and S-III samples: (a) as-synthesized S-I, (b) calcined (873 K) S-I, (c) as-synthesized S-III, (d) calcined (873 K) S-III. * indicates spinning sidebands.

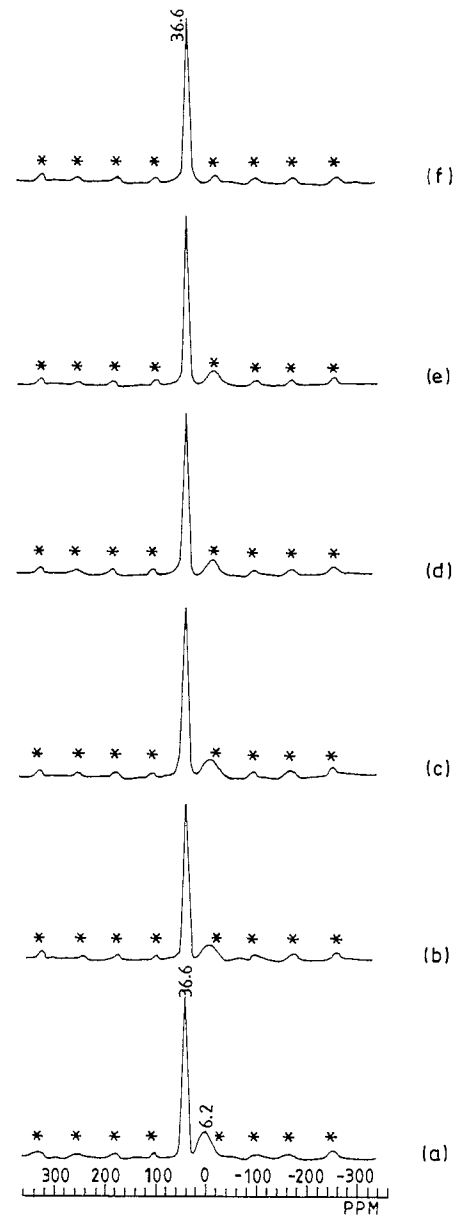

Fig. 8. ^{27}Al MAS NMR spectra of S-II sample calcined at different temperatures: (a) as-synthesized, (b) 473 K, (c) 573 K, (d) 673 K, (e) 773 K, (f) 873 K. * indicates spinning sidebands.

sample, followed by Si(0Al) environment, whereas in the uncalcined species, the intensity of −108 ppm peak corresponding to Si(0Al) species is a maximum. This implies that in S-III sample Si redistributes itself with calcination and gets attached with AlO_4 tetrahedra. This is not very common with other SAPOs. So in both S-II and S-III it is observed that Si(1Al) is the most stable configuration in the calcined samples. From the intensities of the peaks, the relative abundance of Si in different environments for the calcined S-III sample can be given as follows:

$$Si(1Al) > Si(2Al) > Si(3Al) > Si(0Al) > Si(4Al)$$

However in S-II sample the trend is:

$$Si(1Al) > Si(2Al) > Si(0Al) > Si(3Al) > Si(4Al).$$

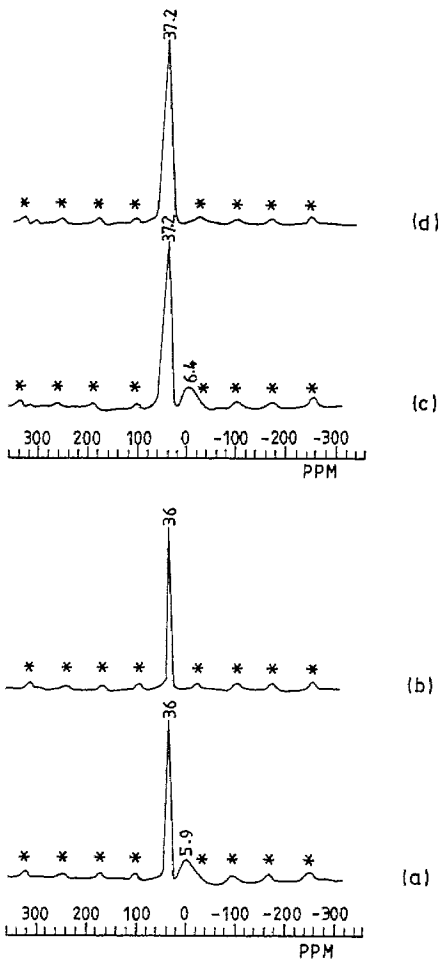

Fig. 9. ^{27}Al MAS NMR spectra of S-I and S-III samples: (a) as-synthesized S-I, (b) calcined (873 K) S-I, (c) as-synthesized S-III, (d) calcined (873 K) S-III. * indicates spinning sidebands.

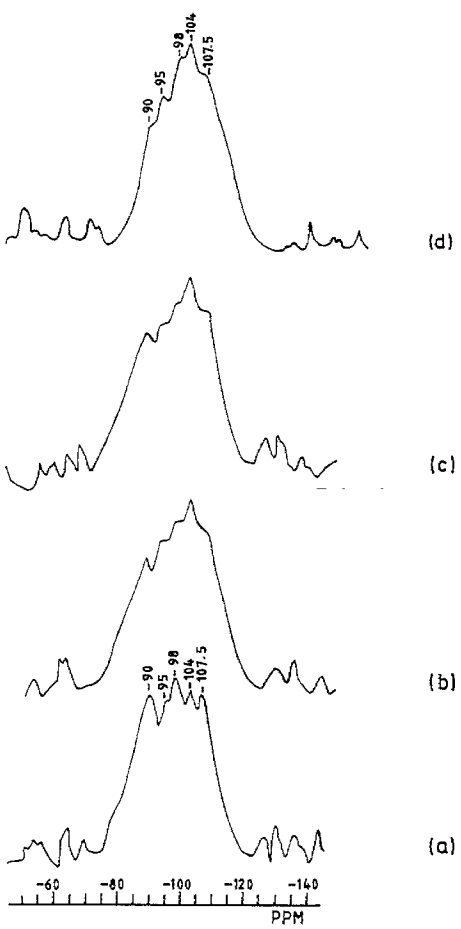

Fig. 10. ^{29}Si MAS NMR spectra of S-II sample calcined at different temperatures: (a) as-synthesized, (b) 673 K, (c) 773 K, (d) 873 K.

Thus, in the synthesized mesoporous SAPO samples, Si is present in multiple environments with Si-rich regions predominating. Also, with increase in the extent of Si incorporation, the concentration of absolute silica islands i.e. Si(0Al) is found to decrease. However, the extents of Si incorporation with more Al neighbors in these mesoporous samples are less compared to other known SAPOs. A similar analogy can be drawn in this respect between the mesoporous aluminosilicates and the known zeolites like HY, HZSM-5, Hβ etc. The framework aluminum in mesoporous aluminosilicates(MCM-41) is found to be less stable than that in zeolites and it comes out of the framework with calcination [11]. Thus acidity in MCM-41 is less compared to other acidic zeolites [12]. A detailed study is in progress for the determination of acidity of these mesoporous SAPOs, which will be communicated shortly.

4. Conclusion

Silicoaluminophosphates in the mesoporous range with varying amounts of silicon incorporation were synthesized. XRD, Sorption studies reveal characteristics of mesoporous material. Solid state MAS NMR spectroscopic studies reveal that Al and P atoms in the

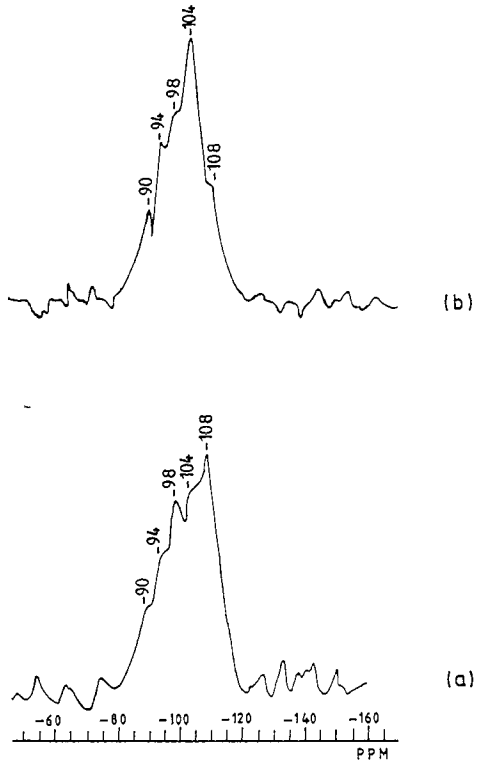

Fig. 11. ^{29}Si MAS NMR spectra of S-III sample: (a) as-synthesized, (b) calcined (873 K).

calcined material are in the tetrahedral environment and silicon redistributes in the lattice on calcination. Probably in these materials no Si–O–P linkage is present. Also, silica-rich regions are found in larger proportions compared to known SAPOs. Si(1Al) environment gives a peak of maximum intensity in ^{29}Si MAS NMR, irrespective of the amount of Si present in the sample. This is a not a common observation in the other known SAPOs. It is also found that Si substitutes P randomly in a heterogeneous manner.

Acknowledgements

The authors wish to thank R.S.I.C. Madras for recording the NMR spectras. The financial assistance received from the Council for Scientific and Industrial Research, India, and the Department of Science and Technology, India, is gratefully acknowledged.

References

[1] M.E. Davis, C. Saldarriaga, C. Montel, J. Garces, C. Crowder, Nature 331 (1988) 698.
[2] Q. Huo, R. Xu, S. Li, Z. Ma, J.M. Thomas, R.H. Jones, A.M. Chippindale, J. Chem. Soc. Chem. Commun., (1992) 875.
[3] C.T. Kresge, M.E. Leonowicz, W.J. Roth, J.C. Vartuli, J.S. Beck, Nature 359 (1992) 710.
[4] B. Chakraborty, A.C. Pulikottil, S. Das, B. Viswanathan, J. Chem. Soc. Chem. Commun., (1997) 911.
[5] Z. Luan, H. He, W. Zhou, C. Cheng, J. Klinowski, J. Chem. Soc. Faraday Trans. 91 (1995) 2955.
[6] E. Jahn, D. Muller, K. Becker, Zeolites 10 (1990) 151.
[7] D. Muller, E. Jahn, B. Fahlke, G. Ladwig, U. Haubenreisser, Zeolites 5 (1985) 53.
[8] C.S. Blackwell, R.L. Patton, J. Phys. Chem. 92 (1988) 3965.
[9] J.A. Martens, C. Jansens, P.J. Grobet, H.K. Beyer, P.A. Jacobs, Zeolites: Facts, Figures, Future, in: P.A. Jacobs, R.A. van Santen (Eds.), Elsevier Sci Pub., Amsterdam, (1989) 215.
[10] S. Ashtekar, V.V. Satyanarayana Chilukuri, D.K. Chakraborty, J. Phys. Chem. 98 (1994) 4878.
[11] Z. Luan, C.F. Cheng, H. He, J. Klinowski, J. Phys. Chem. 99 (1995) 10590.
[12] M.J. Climent, A. Corma, S. Iborra, M.C. Navarro, J. Primo, J. Catal. 161 (1996) 783.